Agricultural and Forest Meteorology 301–302 (2021) 108342

Contents lists available at ScienceDirect

Agricultural and Forest Meteorology

journal homepage: www.elsevier.com/locate/agrformet

Adaptive versus non-adaptive responses to drought in a non-native riparian tree / shrub, *Tamarix* spp

Susan E Bush [a], Jessica S Guo [b], Donna Dehn [a], Kevin C Grady [c], Julia B Hull [d], Emily Johnson [d], Dan F Koepke [a], Randall W Long [e], Dan L Potts [f], Kevin R Hultine [a,*]

[a] Department of Research, Conservation and Collections, Desert Botanical Garden, Phoenix, AZ 85008, USA
[b] Department of Geology and Geophysics, University of Utah, Salt Lake City, UT 84112, USA
[c] School of Forestry, Northern Arizona University, Flagstaff, AZ 86011, USA
[d] Department of Biological Sciences, Northern Arizona University, Flagstaff, AZ 86011, USA
[e] Department of Research and Conservation, Holden Forests and Gardens, Kirtland, Ohio 44094, USA
[f] Biology Department, SUNY Buffalo State, Buffalo, NY 14222, USA

ARTICLE INFO

Keywords:
Hydraulic architecture
local adaptation
plant water relations
riparian ecohydrology
sap flux
stomatal regulation

ABSTRACT

Rapidly colonizing species often thrive in a wide-range of conditions due to a high degree of phenotypic plasticity that results in populations of "general purpose" genotypes. Alternatively, species with high genetic variation could rapidly respond to forces of selection such that a local population evolves traits that provide an advantage in its local environment. We tested this generalist versus local adaptation paradigm in a widely distributed, recently introduced riparian tree / shrub, *Tamarix* spp. Using an eighty-day, mid-summer common garden drought experiment, we tested three inter-related hypotheses: 1) stomatal sensitivity to soil water depletion is lower in genotypes from a low-elevation, ephemerally flowing river than genotypes from a low-elevation, perennially flowing river, indicative of local adaptation to hydrological conditions, 2) stomatal sensitivity to soil water depletion is lower in genotypes from high-elevations with regular freeze-thaw exposure than genotypes sourced from locations with no freeze-thaw exposure, indicative of local adaptation to temperature conditions, and 3) differences among genotypes in drought sensitivity are correlated with differences in fine root area to leaf area ratios (A_r:A_l). For the most part, results did not support hypothesis 1, but largely supported hypotheses 2 and 3. Specifically, sap-flux scaled canopy transpiration (E_l) declined 14 days earlier in the low-elevation populations after drought initiation compared to E_l of the highest elevation population with the highest freeze-thaw exposure. Root area to leaf area ratios of the two low-elevation populations were also only 42% and 55% of A_r:A_l in the highest elevation population. Results indicate that the high degree of reported *Tamarix* hybridization since its introduction to North America has largely produced a swarm of "generalist" genotypes in terms of drought sensitivity. Nevertheless, rapid changes in ecohydrologic conditions may result in some *Tamarix* populations becoming maladapted sooner to reductions in available water than others in the western US.

1. Introduction

Biological invasions are widely recognized as one of the most pressing issues in global change ecology. Yet the evolutionary factors that allow introduced species to successfully establish into new ecosystems and become widespread is not well understood. It is often assumed that rapidly colonizing species that thrive in a wide-range of environmental conditions do so through a high degree of phenotypic or developmental plasticity. A species comprised of highly plastic "general purpose genotypes" (Baker, 1965) may be able to flourish in widely divergent ecosystems, perhaps explaining the success of many invasive plant species (Parker et al., 2003). Alternatively, the rapid expansion of introduced species across broad environmental gradients may be facilitated by rapid local adaptation (Parker et al., 2003; Kawecki and Ebert, 2004). Specifically, species with populations that possess high genetic variation could rapidly respond to forces of selection such that a local population evolves traits that provide an advantage under its local environment (Thompson, 1998; Kawecki and Ebert, 2004). Factors that

* Corresponding Author: phone: 1.480.481.8195
E-mail address: khultine@dbg.org (K.R. Hultine).

https://doi.org/10.1016/j.agrformet.2021.108342
Received 26 May 2020; Received in revised form 19 November 2020; Accepted 21 January 2021

Table 1
Mean elevation, coordinates, mean minimum temperature, mean maximum temperature, approximate number of freeze days per year following warm days absent of freezing, and river flow patterns at locations where *Tamarix* cuttings were sourced from and established in an experimental common garden near Yuma, Arizona.

Source population	Elevation (m)	Latitude	Longitude	Min temp. (°C)	Max temp. (°C)	Freeze-thaw days	River reach
Common garden	58	32.615	-114.636	6.1	41.5	0.00	NA
Colorado R.	48	32.823	-114.485	6.3	41.7	0.00	Perennial
Gila R.	133	32.962	-113.305	4.1	41.7	0.06	Ephemeral
Verde R.	942	34.573	-111.856	-1.9	38.0	8.22	Perennial
Little Colorado R.	1643	34.648	-109.706	-6.4	33.3	34.33	Intermittent

could promote rapid adaptation to local environments - aside from a high genetic diversity - include a high degree of outcrossing and the occurrence of several independent introduction events (Parker et al., 2003). However, rapid adaptation could also be suppressed by genetic drift (Kawecki and Ebert 2004), clonal reproduction or hybridization (Baker, 1965; 1995).

Tamarix is one of the most successful invasive woody plants in North America, with a range from southwestern Canada to northern Mexico. It was brought to North America through multiple introductions starting in the mid 19th century for its horticultural value as well as for erosion and wind control (Long et al., 2017), and neither the genus nor the family, Tamaricaceae, is native to the Western Hemisphere (Horton, 1977). In its native locations, distinct separation in geographical range distribution and morphology has allowed for simple identification of *Tamarix* species that were ultimately introduced to North America (Gaskin, 2003). The two most widely distributed species in North America, *T. ramosissima* Ledeb. and *T. chinensis,* Lour. are generally considered a single aggregate species (Allred, 2002), reflecting molecular analysis revealing that as much as 85% of *Tamarix* found naturalized in the United States are a mosaic of hybrids between *T. ramosissima* and *T. chinensis* (Gaskin and Kazmer, 2009), hereto referred as *Tamarix*.

An important feature of *Tamarix* is that it occurs over extremely broad climate gradients that are punctuated by occasional spring freezing events following leaf flush at high latitude / elevation locations to temperatures that often exceed 45°C during mid-summer in the lower deserts of the southwestern US and northern Mexico. Its distribution is generally limited to wetlands and riparian floodplains, and a recent population genomics analysis suggests that there is a high degree of genetic connectivity within river networks (Lee et al., 2018). The high apparent gene flow (Lee et al., 2018) coupled with significant hybridization following introduction in North America (Gaskin and Schaal, 2002) suggests that *Tamarix* populations are comprised primarily of highly plastic, general-purpose genotypes (Baker, 1965). However, studies using common gardens and glasshouse trials report some traits may be locally adapted across temperature gradients including foliage phenology (Friedman, et al., 2011; Long et al., 2017), cold hardiness (Friedman et al., 2008), biomass allocation (Sexton et al., 2002 2002; Williams et al., 2014), and leaf-level gas exchange (Long et al., 2017).

The riparian habitats in which *Tamarix* thrives are undergoing dramatic shifts in ecohydrology and ecosystem processes. These shifts are largely caused by intensive land use activities coupled with climate change that are having profound impacts on the water cycle in the southwestern US and northern Mexico, and these impacts are anticipated to accelerate over the next several decades. Specifically, the combination of early snow melt and spring runoff (Mote et al., 2005, 2018), higher atmospheric temperatures (Seager et al., 2007), and a higher frequency and intensity of episodic droughts (Seager and Vecchi, 2010) are expected to reduce the discharge of water into streams, rivers and aquifers and thus reduce the availability of soil moisture to riparian vegetation. Whether changes in soil moisture impact the water budget of *Tamarix* equally across its climate niche in North America is an open question. If indeed extensive hybridization has led to a broad swarm of general-purpose genotypes across its range, then perhaps *Tamarix* populations will express a general response to soil water deficits regardless of location. However, evidence for local adaptation in a wide range of functional traits suggests that soil water deficits will not have an equal impact on *Tamarix* water relations, growth and fitness across its range (Sexton et al., 2002; Williams et al., 2014; Hultine et al., 2020).

The focus of this investigation was to experimentally tease apart whether there is a directional response in *Tamarix* genotypes to soil water deficits. We measured stem sap flux, sap flux-scaled canopy transpiration and stomatal conductance, xylem water potential, carbon isotope ratios in leaf soluble sugars and fine root area to leaf area ratios of mature *Tamarix* plants exposed to experimental drought in a common garden setting. The following hypotheses were tested: 1) *Tamarix* genotypes sourced from a low-elevation, ephemerally flowing river reach are more tolerant to the effects of soil water depletion than genotypes sourced from a low elevation, perennially flowing, river reach, indicating a high degree of local adaptation to soil water conditions, 2) *Tamarix* genotypes sourced from high-elevation locations with regular freeze-thaw events are more tolerant to the effects of soil water depletion than genotypes sourced from low-elevation locations with no regular freeze thaw events, indicating a high degree of local adaptation to temperature conditions, and 3) differences among genotypes in drought sensitivity are correlated with differences in population-level fine-root area to leaf area ratios. The experimental design allowed us to separately evaluate potential adaptive (ephemeral versus perennial flowing reaches) versus non-adaptive, correlative trait responses (freezing tolerance versus non-freezing tolerance) to soil water deficits. Results from this investigation provides a stronger understanding of how rapidly changing riparian ecohydrological conditions impact *Tamarix* water relations across large climatic gradients, and more broadly increases understanding of potential rapid evolution in recently introduced plant species.

2. Materials and methods

2.1. Common garden and collections from source populations

The common garden was located at the University of Arizona Mesa Facility, in Yuma, AZ (lat. 32.615 °N, long. -114.636 °W, elev. 60 m) in the southwestern corner of Arizona in the Sonoran Desert. The site is a former agricultural field that was fallow for several years prior to use. The field was tilled and leveled prior to planting to facilitate even flood irrigation. Soils were classified by the soil conservation service as superstition sand, and were comprised of approximately 90% sand, and 5% clay. The climate is typically hot, with dry summers interrupted by rare monsoonal precipitation, and cool winters. *Tamarix* cuttings were collected from 16 source populations located throughout Arizona and southern Utah. Sites were selected across a broad altitudinal gradient (45 – 1791 m) that served as a proxy for both minimum cold temperatures (range: -6.4 - 6.3°C), and maximum hot temperatures (range; 32.4 - 42.4°C).

Cuttings were collected from 16 individual genotypes in each of the 16 populations in the fall of 2014. Cuttings were treated with root hormone, and grown in a vermiculite/perlite potting mix in 328 cm^3 pots at the Northern Arizona University greenhouse facility in Flagstaff, Arizona for four to five months. The potted individuals were transplanted in the common garden in Yuma in April of 2015. Populations were planted in a randomized block design, with each population being

represented once in a total of eight replicate blocks. For each population in each replicate block, a plot of 16 individuals were assigned a random location in a 4 × 4 plant arrangement with 2 m spacing between rooted plants. All of the blocks were regularly watered with flood irrigation on a weekly basis throughout the spring, summer and fall prior to the drought experiment implemented during the summer of 2016 (see below). By August of 2016, all of the trees were multi-stemmed and greater than 2 m tall.

Of the 16 original populations, four were chosen for intensive measurement of drought responses based on contrasts in fluvial hydrology and PRISM-derived climate parameters (PRISM Climate Group 2015). These parameters included mean minimum and maximum temperatures and the number freeze-thaw days that can induce freeze-thaw xylem cavitation (Sperry and Sullivan, 1992) and canopy dieback. Two populations were sourced from sites in the northern Sonoran Desert that are largely absent of freeze-thaw conditions during diurnal cycles (Table 1). One population occurred along the perennially flowing Colorado River near Yuma, AZ, (labeled Col) while the second population was sourced along the lower Gila River (labeled Gila) approximately 50 km west of the city of Gila Bend in central Arizona. The lower Gila River is generally dry year around with occasional episodic flow events that occur following unusually large precipitation events (usually in winter). The other two populations were sourced from river reaches on the Colorado Plateau (Table 1). One source population occurred along the perennially flowing Verde River (labeled Verde) near the city of Camp Verde in north central Arizona where it is exposed to seasonal freezing temperatures and, on average 8.22 freeze-thaw days per year. The second high-elevation population occurred along the Little Colorado River (labeled LC) approximately 40 km northwest of the town of St Johns., AZ. Following the end of snow-melt, this reach of the Little Colorado often ceases to flow in the late spring and resumes flowing with the onset of mid-summer monsoon thunderstorms. Genotypes at this high-elevation site are exposed to on average 34.33 freeze-thaw days per year (Table 1).

2.2. Drought experiment, soil moisture and micrometeorology

Following flood irrigation on August 1, 2016 (Julian day 214), irrigation was ceased for half of the common garden for the duration of the study. One 16-tree plot within the drought-treated half of the garden was randomly selected per population, and 10 of the 16 trees within each selected plot were randomly selected for intensive study of physiological drought responses. Percent volumetric soil moisture (θ) was measured continuously at depths of 15 cm and 45 cm under three randomly selected canopies with CS616 Water Content Reflectometer Probes (Campbell Scientific, Logan, UT, USA). Photosynthetic active radiation, air temperature and humidity were measured continuously from a micrometeorological station located on site. Above-canopy photosynthetic active radiation (Q) was measured with an Apogee SQ-110-SS sun calibration quantum Sensor (Apogee Instruments, Logan, UT, USA). Temperature and humidity were measured with a shielded Vaisala HMP 60 AC temperature / humidity probe (Vaisala, Woburn, MA, USA) placed 3 m above the ground surface. Soil moisture and micrometeorology data were measured every 30 s and stored as 30 min averages from July 25 (day 207) to Oct 18 (day 292) with a Campbell CR10X-2M data logger (Campbell Scientific, Logan, UT, USA). Measurements of temperature and humidity were used to calculate atmospheric vapor pressure deficit (D).

2.3. Xylem water potentials and $\delta^{13}C$ from leaf soluble carbohydrates

Xylem water potentials and carbon isotope ratios of leaf soluble sugars were measured to evaluate plant water status before and after implementation of the drought treatment. Xylem water potentials were measured with a Scholander-type pressure chamber (PMS Instruments, Corvalis, OR, USA) immediately following the final irrigation on August 4 (day 217), and again on August 30 (day 243, 26 days since watering), September 26 (day 270, 63 days since watering) and October 18 (day 292, 75 days since watering) to track variation in water status throughout the drought treatment. A single shoot tip from six of the 10 trees per plot was cut with a sharp razor blade and measured at predawn (Ψ_{pd}) between 02:00 and 04:00 hours and at midday (Ψ_{md}) between 11:00 and 13:00 hours. After cutting, the shoot tips were immediately placed in a sealed ziplock bag with a moist paper towel and measurements were taken approximately 1 to 10 minutes after excising from the tree.

Carbon isotope ratios of soluble leaf carbohydrates ($\delta^{13}C$) were evaluated to infer leaf gas exchange (photosynthesis and stomatal conductance) variability over short time periods (24-72 hrs; Brugnoli et al., 1988; Brugnoli and Farquhar, 1998). 30-40 sunlit leaflets and associated photosynthetic stem tissues were were collected at mid-canopy height after dusk on July 23 (day 205), August 30 (day 243), September 20 (day 264) and October 17 (day 291). These days were selected for leaf collections because they were cloudless, or in the case of day 264, nearly cloudless resulting in near identical levels of Q. The leaves were immediately immersed in liquid nitrogen after collection to inhibit all metabolic activity. The leaves were transported to the lab on dry ice and stored at -80°C.

Leaf soluble carbohydrates were extracted using methods previously reported by Brugnoli et al. (1988) and Hultine et al. (2013). Leaf soluble carbohydrates were extracted in distilled water, followed by a purification procedure according to Brugnoli et al. (1988), and freeze-dried for approximately 72 hrs. In order to insure the repeatability of our extraction approach, we established an "in house" lab standard from *Populus fremontii* leaves that were homogenized and stored at -80°C. A leaf standard sample was extracted along with each subset of *Tamarix* leaves and prepped for $\delta^{13}C$ analysis. Carbon isotope ratios were determined using an elemental analyzer (Model NC2100, Carlo Erba, Milano, Italy) coupled with a Finnigan DELTA Plus Advantage ratio mass spectrometer (ThermoFisher Scientific, Watham, MA, USA) using a continuous flow inlet. The samples were analyzed at the Colorado Plateau Stable Isotope Laboratory at Northern Arizona University, and standardization was based on a broad range of isotope, elemental and secondary standards.

2.4. Sap flux, canopy transpiration and stomatal conductance

Ten trees from each population were instrumented with thermal dissipation sap flux probes (Granier, 1987), where the volumetric flow rate of water through the xylem is empirically related to the temperature difference between a heated and reference sensor probe pair according to:

$$J_s = a\left(\frac{\Delta T_m}{\Delta T} - 1\right)^b \quad (1)$$

where J_s is sap flux density (g m^{-2} s^{-1}), ΔT is the temperature difference between the heated and reference sensors, ΔT_m is the temperature difference between the heated and reference sensors measured under assumed zero-flow conditions during nighttime periods (Granier, 1987), and a and b equal 119 and 1.231 respectively. Each tree was instrumented with 1 cm length stainless steel probes installed at breast height, with axial separation of 15 cm, and where azimuth of sensor placement was randomized. Prior independent, controlled laboratory calibration experiments with *Tamarix* stem material and 1 cm length probe installations yielded slightly different values of 240 and 1.163 for the empirically derived coefficients a and b respectively compared to the original calibration according to Granier (Granier, 1987; Hultine et al., 2010). As a result, the values derived from experiments by Hultine et al. (2010) were used to calculate sap flux density according to equation 1. Measurements were made continuously every 30 seconds throughout the measurement time period, and half-hour means were stored using a

CR1000X datalogger (Campbell Scientific, Logan UT, USA). Following the conclusion of the drought experiment, the entire branch of each sap flux installation was harvested for sapwood area measurements. In all cases, the 1 cm length sensors did not exceed active sapwood depth. Total branch water use was calculated by multiplying calculated sap flux density (g cm^{-2} day^{-1}) by total conducting sapwood area (cm^{-2}) to yield daily branch water use (g day^{-1}).

Canopy transpiration and stomatal conductance were calculated using sap flux density, total sapwood area and leaf area data. Total sapwood area (A_s) for each tree was obtained by collecting a stem cross-section sample at the point halfway between the heated and reference sensor probe placement. Each stem cross-section was imaged, and total sapwood area was calculated using Image J software (https://imagej.nih.gov/ij/). Total leaf area (A_l) was harvested from each branch of all forty trees. A subset of leaf material from each population was used to calculate specific leaf area (SLA, leaf area/dry mass), where Image J software was also used to calculate total area of fresh leaf material for SLA calculations. Total leaf area for each tree was then calculated using the SLA for each population and the total dry weight of harvested leaf material for each tree. A reduction in leaf area was observed over the course of the drought experiment. In order to estimate the drought induced leaf area loss for each population, trees from the same source populations in the portion of the common garden that had continued to receive irrigation were destructively sampled at the time of destructive sampling of sap flux trees. Total leaf areas sampled from continuously irrigated trees were used to generate a population-specific allometric relationship between total leaf area and subtending cross-sectional stem area (Fig. A1). These allometries were applied to sap flux instrumented trees in order to estimate leaf area to sapwood area ratios at the beginning of the drought experiment, and estimate reductions in leaf area as a consequence of the drought treatment (A_l:A_{lref}).

Canopy transpiration (g m^{-2} day^{-1}) was obtained using the total sapwood area to leaf area ratio (A_s:A_l) according to:

$$\boldsymbol{E}_l = \boldsymbol{J}_s \frac{\boldsymbol{A}_s}{\boldsymbol{A}_l} \quad (2)$$

Where E_l is transpiration per unit leaf area, and canopy stomatal conductance was calculated based on a simplified approach suggested by Monteith and Unsworth (1990) and detailed in Ewers et al (2001) as:

$$\boldsymbol{G}_s = \frac{[\boldsymbol{K}_G(\boldsymbol{T})\boldsymbol{E}_l]}{\boldsymbol{D}} \quad (3)$$

Where G_S (mm s^{-1}) is canopy stomatal conductance, K_G is a temperature dependent conductance coefficient (115.8 + 0.4236T, kPa m^{-3} kg^{-1}), and D is the atmospheric vapor pressure deficit (kPa). Given that the canopies of individual trees rarely overlapped, and the extremely low characteristic leaf dimension of *Tamarix* leaves, we assumed that atmospheric decoupling by tree canopies was negligible and subsequently boundary layer conductance was several fold higher than G_S. Due to the observed reduction in leaf area over the course of the drought time period, A_l was not assumed to be a static value in equations 2 and 3. In order to estimate daily leaf area values, we used a linear interpolation between initial, allometrically derived leaf area, and leaf area obtained by destructive harvest at the conclusion of the drought treatment to estimate A_l for any given day (Hultine *et al.*, 2013) during the drought experiment.

2.5. Root distribution patterns

Soil cores were collected with an 8.25 cm diameter telescoping sand auger (AMS Inc., American Falls, ID) in a single well-watered plot per each of the four populations. Nine soil cores were collected in each plot at 20-cm intervals to a depth of 200 cm. Nine additional cores were taken in each plot at 200-220, 240-260, and 280-300 cm. Three trees were randomly selected in each plot and cores were taken directly underneath the tree canopy adjacent to the main stem, at 0.5 m from the main stem, and in the intercanopy, 1.0 m from the main stem of the randomly selected tree and the main stem of the nearest adjacent tree. The direction of sampling from the main stem was also selected at random, except when that direction was towards the edge of a plot. In those cases those directions were not included in the random sample pool. Soil cores were collected in one-gallon ziplock bags where they were transported to the lab and kept in a -20°C freezer. Soil samples were sieved using progressively smaller mesh sizes with a final pass through a 2 mm, No. 10 mesh (Gilson Co., Lewis Center, OH, USA) and the separated roots were kept frozen prior to analysis.

In the lab, all root samples were cleaned and observed under light microscopy in water to confirm identification via morphology. Visual analyses confirmed morphological criteria for identifying *Tamarix* roots included rigidity, color and branching patterns. Approximately one third of the approximately 350 root samples were immersed in distilled water for 24 hours and analyzed for total surface area (A_r) using WinRHIZO version 2012a image analysis software (Regents Instruments Inc., Canada). Analysis included roots separated into three size classes: <1 mm, 1-2 mm, and 2-5 mm. After the roots were analyzed for surface area, they were oven-dried at 60 °C for 48 hours, and weighed to generate an allometric relationship between dry root mass (M_r; g) and A_r (cm^2), yielding: $A_r = 66.26^* M_r^{0.659}$ ($R^2 = 0.70$, Fig. A2). Total plot A_r was calculated by first extrapolating A_r to soil depths where samples were not collected (i.e. 220-240 cm, 260-280 cm) using a linear decay function with depth. Then, the mean plot-specific A_r was multiplied by the total plot surface area (64 m^2) to obtain a whole-plot root area distribution for each 20 cm soil depth increment.

2.6. Statistical analysis and Bayesian modeling

2.6.1. Analysis of xylem water potentials, leaf $\delta^{13}C$, leaf area and allometric equations

Differences among population in Ψ_{pd}, Ψ_{md}, and $\delta^{13}C$ of leaf sugars prior to the onset of the drought treatment and throughout the drought treatment were evaluated using a repeated-measures analysis of variance (MANOVA) where repeated measurements on a given plant constituted the repeated variables. In each MANOVA, source populations were tested as the main effect. Mean differences among populations in relative leaf area were analyzed using one-way ANOVA followed by a post-hoc Tukey-Kramer test. Regression analysis was performed to develop allometric equations between total leaf area and subtending cross-sectional stem area, and fine root surface area and root biomass. Prism 5 (GraphPad Inc., La Jolla, CA, USA) and JMP 8.0 (SAS Institute Inc. Cary, NC, USA) were used for all statistical analysis of xylem water potentials, $\delta^{13}C$, leaf area and allometric equations with $P \leq 0.05$ as the significant level.

2.6.2. Changepoint analysis of drought effects on E_l

Differences in transpiration response to drought across populations was assessed with a hierarchical Bayesian model. A custom Bayesian approach allowed for the changepoint of each population to be determined hierarchically based on the changepoint of each individual tree's E_l. This was necessary to accommodate the experimental design and large variation in E_l behavior that is common when scaling E_l from measurements of stem sap flux. Individual differences in baseline water transport, which may be a function of leaf area, was accounted for by scaling E_l as a fraction of each individual's maximum E_l, such that response variables ranged between 0 and 1. We restricted our analysis between day-of-year 215 to 295, the 80 days following drought initiation, and excluded days for which PAR was below 500. Furthermore, we excluded genotypes for which 30% or more days had missing values, which resulted in 32 genotypes representing 4 populations (N = 7,8,8,9 for Col, Gila, Verde, and LC, respectively).

Daily E_l fraction (E_{frac}) was modeled as a function of days since drought initiation (d). Initial exploration revealed that individuals

generally exhibited two distinct rates of E_{frac} change over time. Therefore, we utilized a piecewise linear regression with unknown transition points, or a Bayesian changepoint model, which estimates the separate slopes of each linear region and location of the changepoint. To define the likelihood of the data, observed E_{frac} values were assumed to be normally distributed, such that for observation *i*:

$$E_{frac,\,i} \sim Normal\left(\mu_{E,i},\ \sigma_E^2\right) \tag{4}$$

where μ_E is the predicted E_{frac} and σ_E^2 describes the observation variance. Next, we modeled μ_E as two linear functions of d that join at the changepoint (x):

$$\mu_{E,\,i} = a_{g(i)} + b_{g(i),\,j_i} \cdot \left(d_i - x_{g(i)}\right) \tag{5}$$

$$j_i = 1 + I\left(d_i \geq x_{g(i)}\right) \tag{6}$$

where a denotes the E_{frac} at x, b represents the rate of change of E_{frac}, and j is an indicator variable denoting the period before (1) or after (2) the changepoint. $I(d \geq x)$ is an indicator function that equals 1 when $d \geq x$ and is 0 otherwise. Finally, the *a, b*, and *x* parameters were allowed to vary by genotype, akin to a random coefficients model, where $g(i)$ indicates genotype g associated with observation i.

To complete the Bayesian model, we specified priors for the unknown parameters, including hierarchical priors for the population level intercept, slopes, and changepoint parameters:

$$a_g \sim Normal\left(\mu_{a,\,p(g)},\ \sigma_{a,\,p}^2\right) \tag{7}$$

$$b_{g,\,j} \sim Normal\left(\mu_{b,\,p(g)j},\ \sigma_{b,\,p,\,j}^2\right) \tag{8}$$

$$x_g \sim Normal\left(\mu_{x,p(g)},\ \sigma_{x,p}^2\right) \tag{9}$$

We assigned relatively noninformative, standard (conjugate) priors to the population-level means such that the $\mu_{a,p}$ and $\mu_{b,p,j}$ terms were assigned normal priors centered at zero with large variance. The population-level changepoint ($\mu_{x,p}$) was given noninformative Uniform (0,80) prior, which spans the duration of the drought experiment. The observation precision ($1/\sigma_E^2$) was assigned a conjugate, relatively noninformative Gamma(0.01, 0.01) prior. The population-level standard deviations ($\sigma_{a,p}$, $\sigma_{b,p,j}$, and $\sigma_{x,p}$) were given folded Student-t priors with a mean of zero, a standard deviation of 10, and a shape parameter of 2 (Gelman, 2006).

G_s sensitivity to D

Population differences in the sensitivity of stomatal conductance (G_s) to vapor pressure deficit (D) was assessed in a hierarchical Bayesian framework. Because individual genotypes demonstrated unique timing of drought responses, we used the genotype-level changepoint estimated from the previous model to categorize the G_s into initial and subsequent drought responses. Thus, we could compare population-level differences in stomatal sensitivity during both phases of drought response.

Whole-plant stomatal conductance (G_s) was modeled as a linear function of the natural log of D. The observed G_s values were assigned a normal distribution, such that for observation i:

$$G_{s,\,i} \sim Normal\left(\mu_{G,\,i},\ \sigma_G^2\right) \tag{10}$$

where μ_G is the predicted G_s and σ_G^2 describes the observation variance. Next, we modeled μ_G as a linear functions of log(D) following an empirical model of stomatal conductance (Oren et al. 1999):

$$\mu_G, i = -m_{g(i),\,k(i)} \cdot \log(D_i) + G_{ref,\,g(i),\,k(i)} \tag{11}$$

where m represents stomatal sensitivity to D, G_{ref} is the reference conductance at $D = 1$ kPa, and k is an indicator denoting whether the observation occurred before or after the changepoint estimated in the previous model. The m and G_{ref} parameters also varied by genotype, where $g(i)$ indicates genotype g associated with observation i.

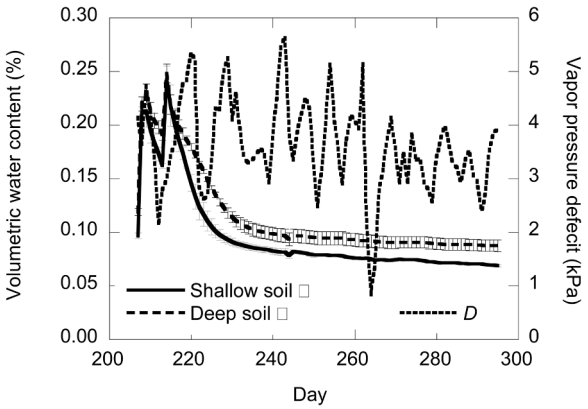

Fig. 1. Mean volumetric water content (θ) measured at 15 cm (shallow soil) and 45 cm (deep soil) depths and mean daytime atmospheric vapor pressure deficit (D) measured 3 m above the ground surface at a *Tamarix* common garden established near Yuma, AZ, USA. Soil moisture data are mean values from sensors installed under three distinct canopies. Error bars represent the standard error of the means.

We specified priors for the unknown parameters, including hierarchical priors for the population level stomatal sensitivity and reference conductance parameters:

$$m_{g,k} \sim Normal\left(\mu_{m,\,p(g),k},\ \sigma_{m,\,p,k}^2\right) \tag{12}$$

$$G_{ref,g,\,k} \sim Normal\left(\mu_{Gref,\,p(g),k},\ \sigma_{Gref,\,p,\,k}^2\right) \tag{13}$$

We assigned relatively noninformative, standard (conjugate) priors to the population-level means such that the $\mu_{m,p,k}$ and $\mu_{Gref,p,k}$ terms were assigned normal priors centered at zero with large variances. The observation precision ($1/\sigma_G^2$) was assigned a conjugate, relatively noninformative Gamma(0.01, 0.01) prior. The population-level standard deviations ($\sigma_{m,p,k}$ and $\sigma_{Gref,p,k}$) were given folded Student-t priors with a mean of zero, a standard deviation of 10, and a shape parameter of 2 (Gelman, 2006).

2.6.3. Model implementation and interpretation

The two Bayesian models (Eqns 4-9 and 10-13) were implemented in JAGS 4.3.0 (Plummer, 2003) via R (R Core Team, 2018), using the packages 'rjags' (Plummer, 2019) and 'CODA' (Plummer et al., 2006). Three parallel Markov chain Monte Carlo (MCMC) sequences were assigned widely dispersed starting values, and initial iterations were run until convergence was achieved as measured by the Gelman statistic (Gelman and Rubin, 1992). We ran each model for 50000 iterations and thinned by 10 to obtain a posterior sample size of 5000 for all parameters.

The above approach produced posterior distributions for all parameters of interest, which are summarized by their posterior means and 95% central credible intervals (CIs) defined by the 2.5 and 97.5 percentiles of the posterior. Significant differences between genotype- and population-level regression coefficients can be determined if the posterior mean of one coefficient is not contained with the 95% CI of another and vice versa. Finally, the difference between population-level stomatal sensitivity (m) and reference conductance (G_{ref}) between the two periods of drought responses were calculated within the model code; Bayesian p-values were calculated to assess the significance of this difference.

3. Results

3.1. Environmental conditions during drought treatment

Mean daytime Q - defined as periods when Q was greater than 10

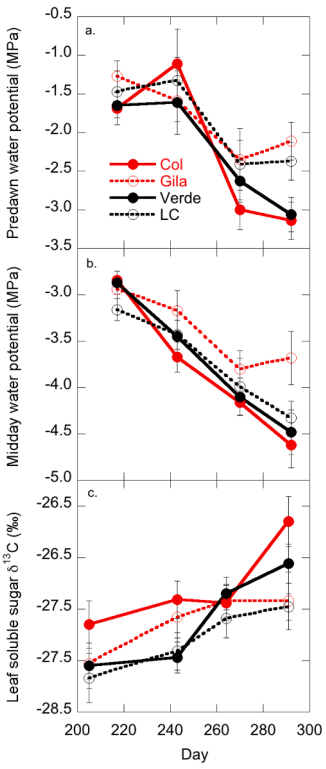

Fig. 2. Mean predawn xylem water potentials (Ψ_{pd}), mean midday xylem water potentials (Ψ_{md}), and carbon isotope ratios ($\delta^{13}C$) of leaf soluble sugars measured in *Tamarix* genotypes sourced from four populations and occurring in a common garden near Yuma, AZ, USA. a. Ψ_{pd} measured between 02:00 and 04:00 hours. b. Ψ_{md} measured between 11:00 and 13:00 hours. c. $\delta^{13}C$ measured in the soluble sugars extracted from sunlit leaves. The population codes are Col (low-elevation, perennial): Colorado River, Gila low-elevation, ephemeral): Gila River, Verde (high-elevation, perennial): Verde River, LC (high-elevation intermittent): Little Colorado River. Error bars represent the standard error of the means.

Table 2
F statistics and *P* values from repeated measures (MANOVA) analysis of predawn xylem water potentials (ψ_{pd}), midday xylem water potentials (ψ_{md}), and carbon isotope ratios of leaf soluble sugars ($\delta^{13}C$). The data were collected prior and and during an experimental drought implemented in a common garden comprised of *Tamarix* genotypes sourced from four populations in Arizona.

Measurement	Population		Time		Pop*Time	
	F	*P*	*F*	*P*	*F*	*P*
Ψ_{pd}	4.20	0.239	40.56	<0.0001	5.52	0.328
Ψ_{md}	5.32	0.113	53.69	<0.0001	4.59	0.177
$\delta^{13}C$	6.16	0.101	16.67	<0.0001	3.66	0.377

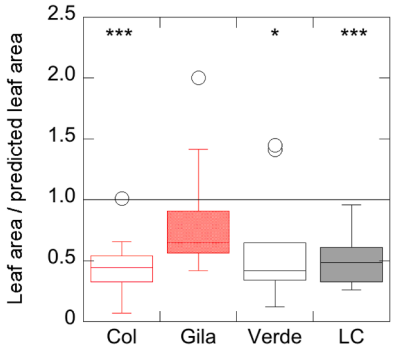

Fig. 3. Box and whisker plot of the ratio of total stem leaf area at the conclusion of the drought experiment and predicted leaf area of *Tamarix* genotypes from four source populations occurring in a common garden near Yuma AZ, USA. Predicted leaf area was determined from an allometric relationship between leaf area and branch diameter calculated for replicated genotypes that were not subjected to the drought treatment. The box and whisker plot shows the median, 25th and 75th percentiles (boxes) and the 10th and 90th percentiles (error bars). The population codes are Col (low-elevation, perennial): Colorado River, Gila low-elevation, ephemeral): Gila River, Verde (high-elevation, perennial): Verde River, LC (high-elevation intermittent): Little Colorado River. Asterisks represent level of significant differences: * < 0.01, ** < 0.001, *** < 0.0001.

μmol m^{-2} s^{-1} – was above 700 μmol m^{-2} s^{-1} every day during the experiment with the exception of three consecutive cloudy days from Sep 21-23 (Julian days 263-265) when mean daytime *Q* only reached 380 – 470 μmol m^{-2} s^{-1}. Likewise, mean daytime *D* on days 264 and 265 only reached 0.80 and 1.37 kPa, respectively. On all other days, *D* ranged from 2.13 kPa to 5.66 kPa (Fig. 1). There was a slight but significant decrease in daytime *D* from the initiation of the drought treatment and the conclusion of the study (Fig. 1, $F_{1,80} = 12.67$, $P = 0.0006$, $R^2 = 0.14$, regression not shown). Mean daily volumetric soil moisture (θ) reached maximum values on the day of flood irrigation (day 214) of 24% and 25% at 15 cm, and 45 cm, respectively (Fig. 1). Mean daily θ decreased rapidly until day 245 when it decreased at both depths linearly from approximately 8.2% to 6.9% at 15 cm, and 9.7% to 8.7% at 45 cm (Fig. 1).

3.2. Xylem water potentials, leaf carbon isotope ratios and whole-canopy leaf area

At the onset of the drought treatment mean Ψ_{pd} of all genotypes was -1.52 (SE ± 0.10) with no significant variation among populations (Fig. 2). On day 292 (Oct 19, 80 days following final watering), mean Ψ_{pd} of all genotypes fell to -2.67 (SE ± 0.14) MPa. However, in contrast to the outset of the drought treatment, differences among population were detected on day 80 after drought initiation, particularly in the low elevation populations where Ψ_{pd} where mean values ranged from -2.11 MPa in the Gila genotypes to -3.14 in the Col genotypes (Fig. 2a). When analyzed across all measurement periods during the drought treatment, no differences were detected among populations (Table 1), although the approximate 1 MPa drop in Ψ_{pd} over the course of the experiment was highly significant (Table 1). The interaction population * time had no effect on Ψ_{pd}.

Similar to Ψ_{pd}, no differences were detected among populations in Ψ_{md} throughout the drought treatment, but time into the drought treatment had a significant effect on Ψ_{md} (Fig. 2b, Table 2). By day 80 into the drought treatment (i.e. day 292), mean Ψ_{md} fell below a threshold that previously has been shown to induce near complete xylem cavitation in the stems in three of the four populations (-4.29 MPa; Pockman and Sperry, 2000; Choat et al., 2012), with the Gila population being the one exception where minimum Ψ_{md} during the experiment only reached -3.68 MPa (Fig. 2b). Patterns of $\Delta\Psi$ (Ψ_{pd} - Ψ_{md}) mirrored patterns of Ψ_{pd} and Ψ_{md} in that mean population differences over the course of the drought treatment were not detected (Table 2, Fig. A3). Time into the drought treatment had a weak, but significant effect on $\Delta\Psi$. However, mean $\Delta\Psi$ across all populations at the conclusion of the experiment was nearly identical to $\Delta\Psi$ at the onset of the experiment: 1.43 (SE ± 0.14) MPa and 1.61 (SE ± 0.09) MPa on days 217 and 292, respectively (Fig. A3).

Patterns of $\delta^{13}C$ in leaf soluble sugars also mirrored patterns of Ψ_{pd}, and Ψ_{md} in that no population differences were detected, but there was a strong effect of time into the drought treatment (Table 2, Fig. 2c). The interaction population * time had no effect on $\delta^{13}C$. Prior to the drought treatment, mean $\delta^{13}C$ of all genotypes was -27.50 (SE ± 0.11) ‰ and increased to -26.66 (SE ± 0.13) ‰ at the conclusion of the drought treatment (Fig. 2c). In contrast to $\delta^{13}C$ patterns that were general across

Table 3
Mean stem sapwood area (A_s), initial leaf area (A_l) - estimated from allometry (Figure S1), and ending leaf area of *Tamarix* genotypes sourced from four populations in Arizona. Numbers in parentheses are ± the standard error of the means.

Population	A_s cm^2	Initial A_l m^2	Ending A_l m^2	Initial A_s:A_l cm^2 m^{-2}	Ending A_s:A_l cm^2 m^{-2}
Colorado	6.60 (0.98)	1.82 (0.34)	0.84 (0.22)	3.81 (0.18)	16.35 (6.77)
Gila	5.92 (0.99)	1.72 (0.39)	1.31 (0.27)	3.73 (0.15)	5.26 (0.67)
Verde	5.17 (0.70)	1.42 (0.23)	0.76 (0.23)	3.78 (0.09)	10.74 (2.85)
Little Colorado	3.73 (0.37)	0.77 (0.08)	0.43 (0.08)	4.84 (0.06)	10.69 (1.46)

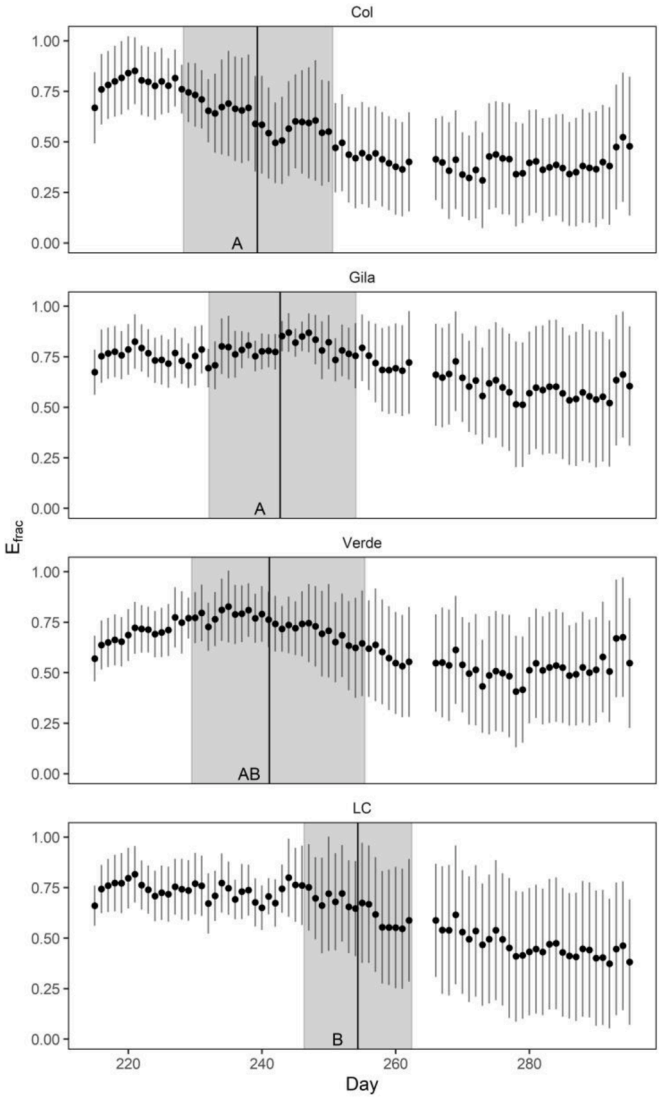

Fig. 4. Mean daily scaled transpiration (E_{frac}, ±1 SD) for the populations Col (n = 7), Gila (n = 8), Verde (n = 8), and LC (n = 9) from day of year 215 to 295, excluding two days when PAR < 500. Vertical line represents the posterior mean of μ_x (i.e. change point) for each population, while the shaded rectangle shows the central 95% credible interval (CI). Capital letters indicate whether μ_x differs significantly among populations.

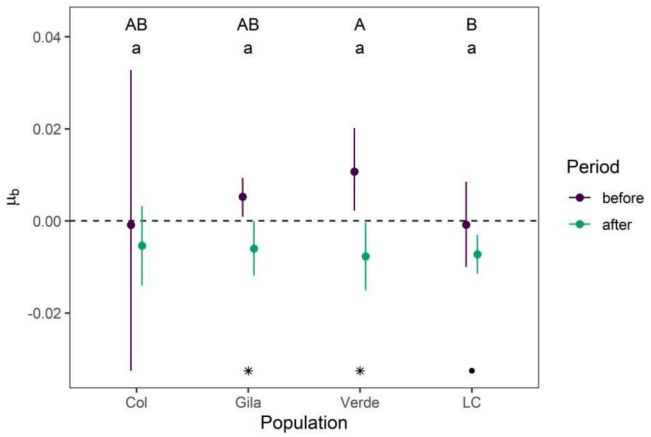

Fig. 5. Posterior mean and central 95% credible interval of μ_b (i.e. slope of leaf transpiration against time after drought initiation) for each population and period. Capital (lowercase) letters indicate whether μ_b differs significantly between populations before (after) the changepoint (μ_x). Asterisks indicate significant differences (Bayesian p-value < 0.01) within a population between periods, while points indicate marginally significant differences (Bayesian p-value < 0.1).

populations, significant differences were detected among populations in A_l:A_{lref}. Genotypes from the perennial flowing Col population displayed the lowest A_l:A_{lref} of 0.45 (SE ± 0.084), followed by the LC population and Verde populations at 0.53 (SE ± 0.070), and 0.59 (SE ± 0.147), respectively (Fig. 3). Conversely, A_l:A_{lref} in the Gila genotypes did not diverge statistically from unity yielding a mean value of 0.88 (SE ± 0.162) (Fig. 3). Consequently, calculated mean A_s:A_l ratios ranged from 3.73 (SE ± 0.15) cm^2 m^{-2} in the Gila population to 4.84 (SE ± 0.06) cm^2 m^{-2} in the LC population at the outset of the drought treatment and ranged from 5.26 (SE ± 0.67) cm^2 m^{-2} in the Gila population to 16.35 (SE ± 6.67) cm^2 m^{-2} in the Col population at the conclusion of the drought (Table 3). However, the extremely high post drought A_s:A_l Col population was largely a function of a single genotype loosing almost all of its leaves. When the tree is removed from the analysis, A_s:A_l fell to 9.99, which was close to the Verde and LC populations.

3.3. Sap-flux-scaled canopy transpiration and canopy stomatal conductance

Sap flux density (J_s) over the seven days prior to the drought treatment was similar among the four populations ranging from a low of 92 (SE ± 6.1) g cm^{-2} day^{-1} in the Gila population to a high of 102 (SE ± 9.6) g m^{-2} s^{-1} in the Verde population with a mean J_s across all genotypes of 97 (SE ± 4.5) g cm^{-2} day^{-1} (Fig A4). At the final seven days of the drought treatment, mean J_s ranged from a low of of 50 (SE ± 14.7) g cm^{-2} day^{-1} in the LC population to a high of 67 (SE ± 16.0) g m^{-2} s^{-1} in the Verde population with a mean J_s across all genotypes of 58 (SE ± 7.5) g cm^{-2} day^{-1} (Fig A4a). Mean canopy transpiration (E_l) during the seven days prior to the drought treatment was 57% and 51% higher in LC than Col, and Gila, respectively, while E_l in Verde population was not significantly different from the other three populations (Figure S4b). Changes in E_l over the course of the drought treatment were more subtle than changes in J_s (Fig. A4b), largely reflecting significant reductions in leaf area (Fig. 3), resulting in higher A_s:A_l ratios by the end of the drought (Table 3).

The decline of E_l over time after drought initiation (d) was nonlinear, largely reflecting confounding effects of variation in D over the course of the drought (Fig. 1). Therefore, we fitted a hierarchical Bayesian model to detect distinct transition points (i.e. changepoints) in mean daily E_{frac} over time (R^2 = 0.86 – 0.91 for each population, Fig. A5). The changepoint – the point in which E_{frac} begins to significantly decline – occurred at about the same day in the Col (day 240, 35

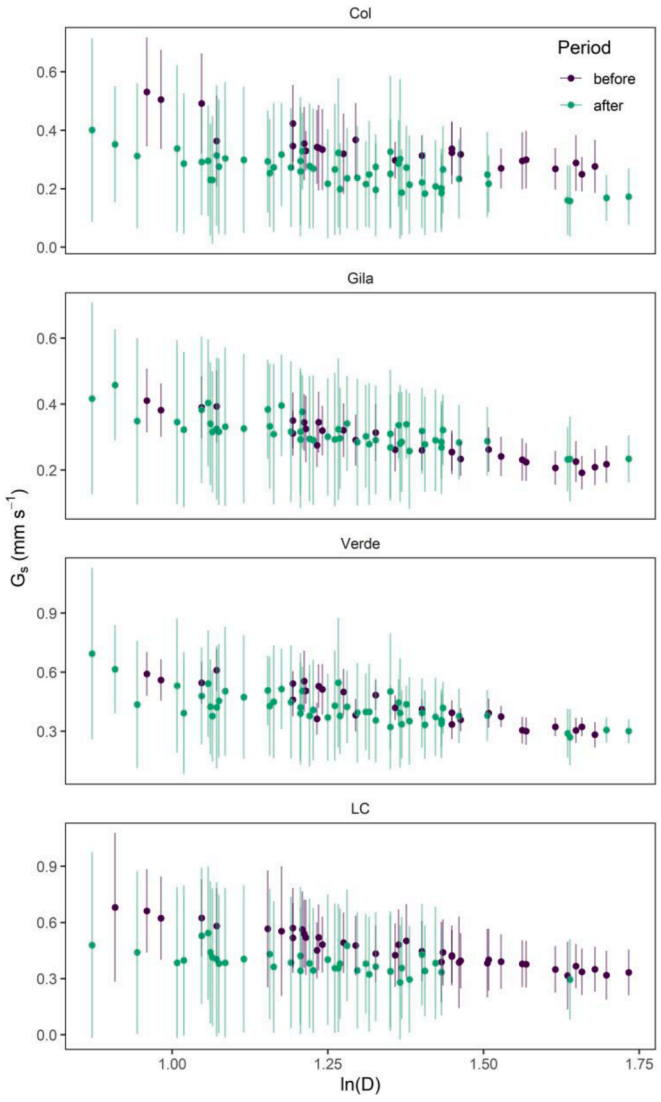

Fig. 6. The relationship between mean daily canopy conductance (G_s, ±1 SD) and natural log of mean daily vapor pressure deficit (D) for each population. The population codes are Col: Colorado River, Gila: Gila River, Verde: Verde River, LC: Little Colorado River.

days after watering), Verde (day 241, 36 days after watering), and Gila (day 242, 37 days after watering) populations (Fig. 4). Conversely, the changepoint occurred on day 254 (49 days after watering) in the LC population: significantly later than either the Col or Gila populations (Fig. 4). Prior to the changepoint, none of the four populations showed a negative slope with d (i.e. μ_b in Fig. 5). In fact, the slopes were initially positive in both the Gila and Verde populations before turning negative after the changepoint (Fig. 5).

To further evaluate stomatal sensitivity to drought, we calculated the relationship between sap-flux-scaled canopy stomatal conductance (G_s) and D before and after the changepoint (Fig. 6) by fitting a hierarchal Bayesian model (R^2 = 0.71 – 0.86, Fig. A6). Prior to the change point, the two high-elevation, frost exposed populations displayed a higher sensitivity to increasing D, illustrated by the larger mean μ_m values in Fig. 7. After the changepoint, G_s become considerably more variable in all populations and no differences were detected among populations (Fig. 7). After the changepoint, G_s in the two low-elevation populations had a marginally lower sensitivity to D than prior to the changepoint. Differences in G_s sensitivity before and after the changepoint were not detected in the two high elevation populations (Fig. 7).

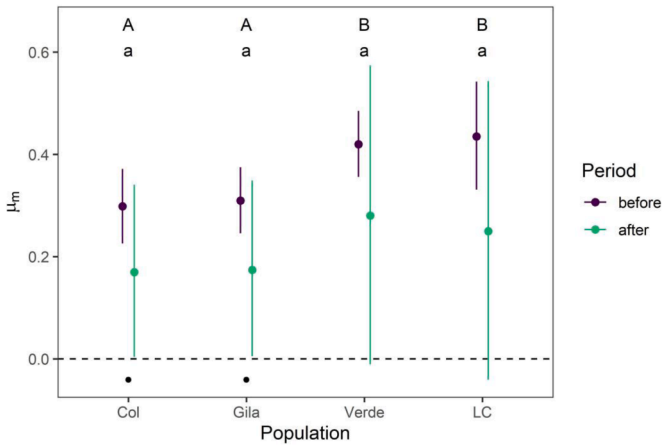

Fig. 7. Posterior mean and central 95% credible interval of μ_m for each population and period. Capital (lowercase) letters indicate whether the parameter differs significantly between populations before (after) the changepoint (μ_x). Points indicate marginally significant differences (Bayesian p-values < 0.1) within a population between periods. The population codes are Col: Colorado River, Gila: Gila River, Verde: Verde River, LC: Little Colorado River.

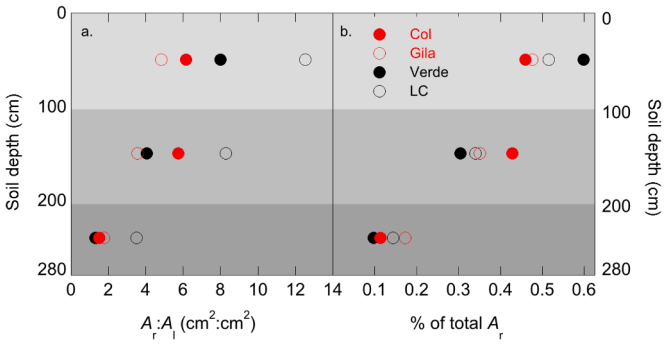

Fig. 8. The fine root distribution of four populations of occurring in a common garden near Yuma, AZ, USA. a. The mean distribution of fine root area relative to total leaf area (A_r:A_l) at three depths: 0 – 100 cm, 100-200 cm, and 200 – 280 cm. b. The percentage distribution of fine roots at three depths: 0 – 100 cm, 100-200 cm, and 200 – 280 cm. The population codes are Col: Colorado River, Gila: Gila River, Verde: Verde River, LC: Little Colorado River

3.4. Fine-root area

From soil depth of 0 to 2.80 m, total A_r:A_l was fairly similar among three of the four populations, ranging from 10.16 m^2 m^{-2} in Gila, to 13.33 m^2 m^{-2} in Verde, to 13.41 m^2 m^{-2} in Col (Fig. 8a). Conversely, A_r:A_l of the LC population was 24.29 m^2 m^{-2}: meaning that A_r:A_l of Gila, Verde and Col were only 42%, 55%, and 55% of LC, respectively (Fig. 8a). The distribution of roots throughout the profile also varied among populations. For example, 60% of the total root area of the Verde population was confined to the upper 1.0 meter of the soil profile. Root area of the Col population was nearly equally distributed between 0 and 1.0 m (46%) and 1.0 to 2.0 m (43%) (Fig. 8b). The Gila population had the highest percentage of its roots below 2.0 m (17%) (Fig. 8b).

4. Discussion

4.1. Adaptive versus non-adaptive responses to drought

The rapid hybridization of *Tamarix* following its introduction in North America (Gaskin and Schaal, 2002; Gaskin and Kazmir, 2009; Williams et al., 2014) suggests that *Tamarix* populations are comprised primarily of highly plastic, general-purpose genotypes (Baker, 1965).

However, common garden studies and glasshouse trials have detected evidence that some traits including foliage phenology (Friedman et al., 2011; Long et al. 2017), cold hardiness (Friedman et al., 2008), biomass allocation (Sexton et al., 2002; Williams et al. 2014), and leaf-level gas exchange (Long et al. 2017) are locally adapted across broad temperature gradients. We therefore anticipated that *Tamarix* populations occurring across both hydrological and mean annual temperature gradients would express strong local adaptation in response to soil water deficits. We found limited evidence that hydrologic regime acts as a strong agent of selection in *Tamarix* populations occurring in low-elevation, arid riparian areas. On the other hand, the population exposed to regular freeze-thaw conditions expressed a delayed negative response in whole-canopy water use to drought that was perhaps a consequence of having a substantially higher A_r:A_l relative to the other three populations. These data indicate that regular exposure to frost may result in a 'non-adaptive' buffering to drought exposure. If so, the occurrence of *Tamarix* in high-elevation riparian ecosystems may have differing ecohydrological, and ecological impacts than *Tamarix* occurring in warmer, low-elevations riparian ecosystems under rapidly changing climate conditions in the western US.

We hypothesized (Hypothesis 1) that the Gila population occurring along an ephemeral stretch of river would express a lower stomatal sensitivity to declining water potentials and a higher A_r:A_l (Hypothesis 3) relative to the Col population sourced along a perennial flowing river. However, we found limited evidence to support either hypothesis, with the exception that unlike the Col population, the Gila population did not display a significant reduction in leaf area by the conclusion of the drought treatment. One limitation is that information on edaphic conditions (i.e. height above primary channel, soil texture), depth to groundwater or other hydrological conditions of the two source locations was absent. Thus, it is plausible that despite the contrasting flow regimes of the two river reaches, the two source populations may have been faced with similar soil water conditions. Alternatively, the results may support the 'generalist genotype' hypothesis (Baker, 1965). A recent genomics analysis of *Tamarix* in the western US revealed that there is high genetic connectivity within large watersheds, including along the lower Colorado River (Lee et al., 2018). The Gila population is located approximately 150 km up river from its confluence with the Colorado River where the Col population is located. *Tamarix* seeds can be dispersed over long distances by water and wind along river corridors (DiTomaso, 1998), making it likely there was significant gene flow between the Col and Gila populations.

We hypothesized that regular exposure to freeze-thaw conditions would result in greater tolerance to drought (Hypothesis 2) due to frost-exposed genotypes having a higher A_r:A_l relative to warm-adapted genotypes (Hypothesis 3). Our second hypothesis was largely supported in that canopy transpiration in the high-elevation LC population declined approximately 14 days after drought initiation than the other three populations (Fig. 4), possibly as a consequence of having a dramatically higher A_r:A_l than the other three populations (Fig. 8). The high A_r:A_l in the cold-adapted LC population may not be an adaptive response to drought *per se* but instead potentially a consequence of coping with winter freezing and regular spring freeze-thaw events. Exposure to freezing requires plants to prioritize frost tolerance through osmoregulation, refilling embolized xylem and frequently rebuilding frost-damaged tissues: processes that require large storage pools of non-structural carbohydrates (Tixier et al., 2019). Another study using the same common garden as the present study found that cold-adapted genotypes maintained higher NSC concentrations in coarse roots than warm-adapted genotypes (Long et al., in revision). Although coarse roots are a primary storage organ for maintaining winter NSC pools in woody plants (Hartmann et al., 2013; Hartmann and Trumbore, 2016; Guo et al., 2020), fine roots may also play an important role NSC storage (Würth et al., 2005). For example, a common garden study revealed that fine roots of cold-adapted species in the genus *Actinidia* - woody taxa native to Asia - contained significantly higher NSC concentrations than fine roots of warm-adapted *Actinidia* species (Boldingh et al., 2000). Other greenhouse / common garden studies have reported that *Tamarix* populations that are regularly exposed to freezing temperatures allocate more biomass to fine root production than genotypes occurring in areas where freezing temperatures are generally absent (Sexton et al., 2002; Williams et al., 2014). Presumably the higher biomass allocation to fine roots in cold-adapted *Tamarix* is a consequence of maintaining labile carbon storage pools, and not necessarily related to soil water deficits.

Plants that are constructed with a higher absorbing root area per unit leaf area have a built in advantage for coping with soil water deficits relative to plants with comparatively low root to leaf area ratios (Sperry and Hacke, 2002; Sperry et al., 2002; Hultine et al., 2006). In the simplest terms, A_r:A_l represents a soil water supply versus atmospheric demand function whereby a large surface area of absorbing roots can not only deliver water to the canopy, but also prevent steep water potential gradients in the rhizosphere and in plant xylem (Sperry et al., 1998). On coarse-textured sandy soils, such as those common in colluvial terraces of riparian systems, A_r:A_l ratios can have considerable impacts on water extraction limits by woody plants. For example, results from a soil / plant hydraulics model (Sperry et al., 1998) indicated that canopy transpiration rates of the semi-arid tree / shrub, *Prosopis velutina* occurring at a location with sandy loam soil was highly sensitive to variation in A_r:A_l. When A_r:A_l was changed from 10 m^2 m^{-2} to 20 m^2 m^{-2} in the model, transpiration increased nearly 100% at the measured bulk soil water potential of -3.5 MPa (Hultine et al., 2006). Thus, in the present study, the high A_r:A_l in the freeze-thaw adapted LC population likely results in greater resilience to soil water deficits relative to other populations, potentially even those occurring in relatively drier environments.

Drought experiments conducted on deeply-rooted, phreatophytic plants can be challenging to implement in ways that are biologically meaningful. Over the 80-day drought treatment in the present study, mean Ψ_{pd} decreases by 1.0 to 1.5 MPa in all populations, mean $\delta^{13}C$ increased by approximately 1.0‰ across all populations (Fig. 2c), and mean G_s became far more variable and less constrained by D (Fig. 7). In three of the four populations, mean Ψ_{md} fell below -4.29 MPa at the conclusion of the drought: a threshold at which near complete hydraulic failure has been previously reported in *Tamarix* (Choat et al., 2012). Interestingly, mean minimum Ψ_{md} in Gila did not fall below the hydraulic failure threshold (Fig. 2c), and was likewise the only population that did not display a significant reduction in leaf area at the conclusion of the drought. Despite the considerable leaf loss in most populations, $\Delta\Psi$ was more or less constant throughout the drought treatment. The near-constant $\Delta\Psi$ indicates that *Tamarix* largely expresses an anisohydric hydraulic strategy that could predispose this taxon to be widely impacted by episodic drought conditions that are predicted to increase in western North America over the next several decades.

4.2. Ecohydrological implications

In order to evaluate the population-level ecohydrological consequences of *Tamarix* on riparian ecosystems it is worth comparing water use strategies and evidence of local adaptation with another widely distributed riparian tree species, *Populus fremontii* S. Wats. In many ways, *P. fremontii* is a native analog to *Tamarix* in that their ranges widely overlap, both have distributions that span broad temperature gradients, and both show strong evidence for local adaptation in traits related to foliage phenology (Friedman et al., 2011, Long et al., 2017; Cooper et al., 2019), cold hardiness (Friedman et al., 2011), productivity (Grady et al., 2011) and photosynthetic gas exchange (Grady et al., 2013; Long et al., 2017). However, a potentially important contrast between *Tamarix* and *P. fremontii* revolves around differences in leaf-level transpiration. In the present study, mean E_l in the freeze-thaw adapted LC population, prior to the drought treatment was over 50% higher than the two low-elevation warm-adapted populations. The relatively high E_l in cold-adapted *Tamarix* likely reflected a much higher

A_r:A_l than warm-adapted *Tamarix*. Conversely, a previous common garden study of *P. fremontii* genotypes sourced across a broad temperature gradient revealed that warm-adapted genotypes had a 35% higher mean E_l than cold-adapted genotypes (Hultine et al., 2020). *P. fremontii* genotypes on the warm-edge of its distribution are faced with the challenge of maximizing thermal regulation of their broad sun-exposed leaves that in absence of significant mid-afternoon evaporative cooling could face rapidly diminishing returns on investment in terms of leaf carbon balance (Urban et al., 2017; Blonder and Michaletz, 2018). On the other hand, the small scale-like leaves of *Tamarix* likely do not require extreme evaporative cooling to the extent that low-elevation *P. fremontii* and some other warm-desert woody taxa are adapted to maintain during heat waves (Aparecido et al., 2020).

Unfortunately, to our knowledge drought treatments similar to the one conducted in the present study have not been conducted on a wide range of western North America riparian tree taxa. As a consequence, the extent to which riparian tree populations are locally adapted to drought conditions across broad climate gradients is an open question. An improved understanding of genetics-based local adaptation in relation to soil water deficits would significantly improve climate niche modeling (Ikeda et al., 2016), and restoration efforts to not only manage non-native vegetation such as *Tamarix*, but also restore native riparian vegetation using assisted migration approaches (Grady et al., 2015).

5. Conclusions

Results from this common garden drought experiment indicate the rapid expansion of *Tamarix* into western north America was likely not facilitated by local adaptation to variation in soil water deficits. However, local adaptation to regular freeze-thaw exposure may have 'non-adaptive' consequences on tolerance to soil water deficits through selection for high belowground versus aboveground biomass allocation, yielding relatively large A_r:A_l ratios. Results from this study improve our understanding of how *Tamarix* has successfully established across an extremely broad climate gradient, and also builds on our understanding of the impacts *Tamarix* may have on ecohydrological processes under future climate conditions. More broadly, the results from this study contribute to our understanding of the "general purpose genotype" versus rapid local adaptation paradigm in successfully established non-native woody plants. It appears that *Tamarix* cannot be neatly classified into either category but instead takes on a myriad of evolutionary strategies to maintain its dominant presence along many wetlands, streams and rivers in western North America.

Declaration of Competing Interest

The authors declare that they have no known competing financial interests or personal relationships that could have appeared to influence the work reported in this paper.

Acknowledgements

Financial support was provided by a grant from the National Science Foundation's (Grant # 1340856) MacroSystems Biology program awarded to KRH and a grant from the US Department of Agriculture, National Institute of Food and Agriculture (Grant # 2015-67013-12138) awarded to KRH. We thank S. Carey, C. Hunyh, T Nguyen, L. Strander and A. VanKirk for their invaluable assistance in the field and in the lab.

Appendix

Fig. A1, A2, A3, A4, A5, A6

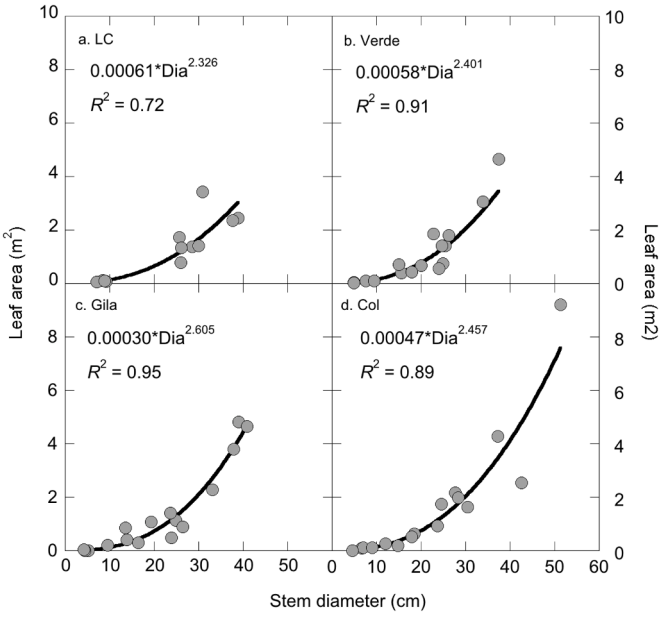

Fig. A1. Population-specific allometric relationships between leaf area and stem diameter. The population codes are Col (low-elevation, perennial): Colorado River, Gila low-elevation, ephemeral): Gila River, Verde (high-elevation, perennial): Verde River, LC (high-elevation intermittent): Little Colorado River.

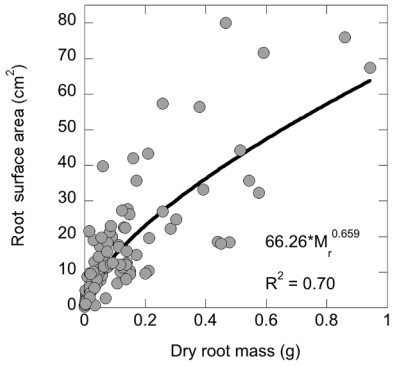

Fig. A2. Allometric relationship between root surface area and root dry mass in fine roots extracted from between 0 and 280 cm.

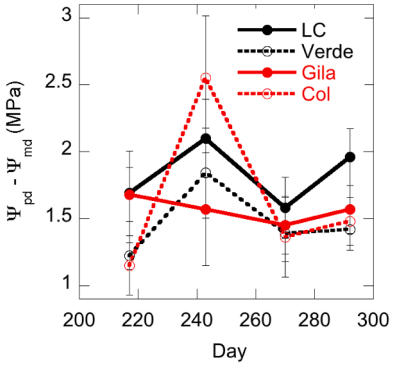

Fig. A3. Mean difference between predawn xylem water potentials (Ψ_{pd}) and mean midday xylem water potentials (Ψ_{md}) measured in *Tamarix* genotypes sourced from four populations and occurring in a common garden near Yuma, AZ, USA. The population codes are Col: Colorado River, Gila: Gila River, Verde: Verde River, LC: Little Colorado River. Error bars represent the standard error of the means.

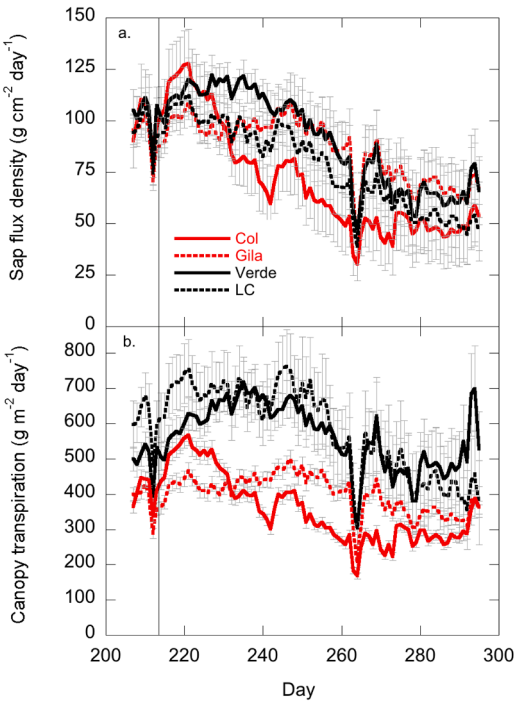

Fig. A4. Mean sap flux density (a) and sap-flux-scaled canopy transpiration (b) measured from July 26 (Day 207) to Oct 22 (Day 295), 2016. The vertical line represents the final flood irrigation during the experiment on August 1 (Day 213). The population codes are Col: Colorado River, Gila: Gila River, Verde: Verde River, LC: Little Colorado River. Error bars represent the standard error of the means.

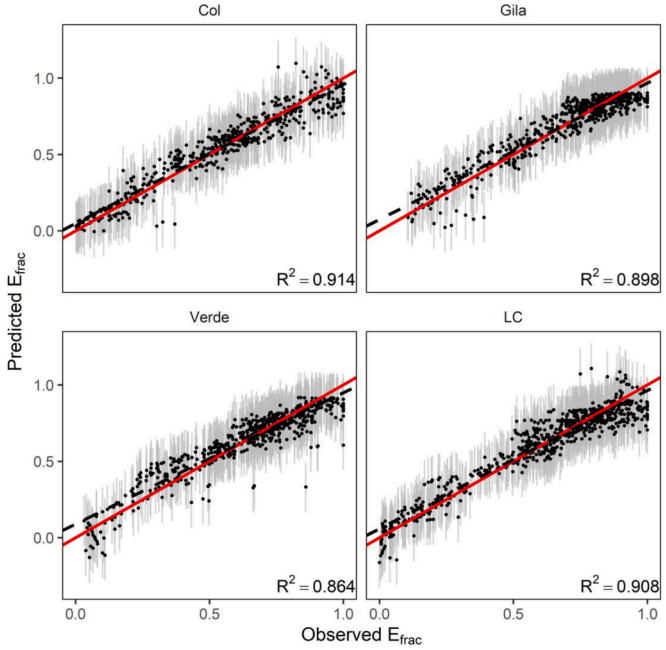

Fig. A5. Predicted versus observed E_{frac} for each population (overall R^2 = 0.90). The red line is the 1:1 line, and the dotted line represents the line of best fit. The population codes are Col: Colorado River, Gila: Gila River, Verde: Verde River, LC: Little Colorado River. Error bars represent the standard error of the means.

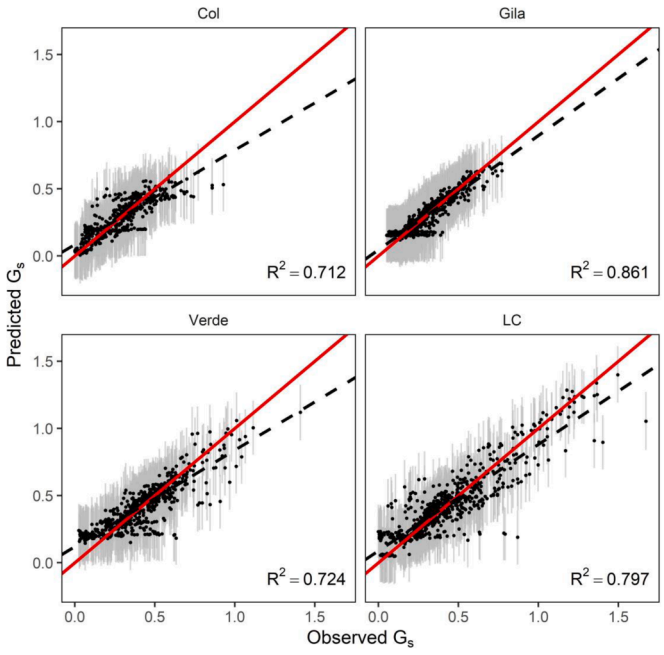

Fig. A6. Predicted versus observed G_s for each population (overall R^2 = 0.80). The red line is the 1:1 line, and the dotted line represents the line of best fit. The red line is the 1:1 line, and the dotted line represents the line of best fit. The population codes are Col: Colorado River, Gila: Gila River, Verde: Verde River, LC: Little Colorado River. Error bars represent the standard error of the means.

References

Allred, K.W., 2002. Identification and taxonomy of (Tamaricaceae) in New Mexico. Desert Plants 18, 26–32.

Aparecido, L.M.T., Woo, S., Suazo, C., Hultine, K.R., Blonder, B, 2020. High water use in desert plants exposed to extreme heat. Ecol. Lett. (In press).

Baker, H.G., 1965. Characteristics and modes of origin of weeks. In: Baker, H.G., Stebbins, G.L. (Eds.), The genetics of colonizing species. Academic Press, New York.

Baker, H.G., 1995. Aspects of the genecology of weeds. In: Kruckeberg, A.R., Walker, R. B., Leviton, A.E. (Eds.), Genecology and ecogeographic races. American Association for the Advancement of Science, San Francisco.

Blonder, B., Michaletz, S.T., 2018. A model for leaf temperature decoupling from air temperature. Agric. For. Meteorol. 262, 354–360.

Boldingh, H., Smith, G.S., Klages, K., 2000. Seasonal concentrations of non-structural carbohydrates of five *Actinidia* species in fruit, leaf and fine root tissue. Ann. Bot. 85, 469–476.

Brugnoli, E., Hubick, K.T., von Caemmerer, S., Wong, S.C., Farquhar, G.D., 1988. Correlation between carbon isotope discrimination and leaf starch and carbohydrates of C_3 plants and the ratio of intercellular and atmospheric partial pressures of carbon dioxide. Plant Physiol 88, 1418–1424.

Brugnoli, E., Farquhar, G.D., 1998. Photosynthetic fractionation of carbon isotopes. In: Leegood, R.C., Sharkey, T.D., von Caemmerer, S. (Eds.), *Photosynthesis: Physiology and Metabolism, Advances in Photosynthesis*. Kluwer Academic Publishers, Dordrecht, pp. 399–434.

Choat, B., et al., 2012. Global convergence in the vulnerability of forests to drought. Nature 491, 752–756.

Cooper, H.F., Grady, K.C., Cowan, J.A., Best, R.J., Allan, G.J., Whitham, T.G., 2019. Genotypic variation in phenological plasticity: reciprocal common gardens reveal adaptive responses to warmer springs but not to fall frost. Glob. Change Biol. https://doi.org/10.1111/gcb.14494.

DiTomaso, J., 1998. Impact, biology, and ecology of saltcedar (Tamarix spp.) in the southwestern United States. Weed Tech 12, 326–336.

Ewers, B.E., Oren, R., Phillips, N., Stromgren, M., Linder, S., 2001. Mean canopy stomatal conductance responses to water and nutrient availabilities in *Picea abies* and *Pinus taeda*. Tree Physiol 21, 841–850.

Friedman, J.M., Roelle, J.E., Gaskin, J.F., Pepper, A.E., Manhart, J.R., 2008. Latitudinal variation in cold hardiness in introduced *Tamarix* and native *Populus*. Evol. Appl. 1, 598–607.

Friedman, J.M., Roell, J.E., Cade, B.S., 2011. Genetic and environmental influences on leaf phenology and cold hardiness of native and introduced riparian trees. Int. J. Biomet. 55, 775–787.

Gaskin, J.F., Schaal, B.A., 2002. Hybrid *Tamarix* widespread in US invasion and undetected in native Asian range. Proc. Nat. Acad. Sci. 99, 11256–11259.

Gaskin, J.F., 2003. Molecular systematics and the control of invasive plants: A case study of *Tamarix* (Tamaricaceae). Ann. Rev. Mis. Bot. Gar. 90, 109–118.

Gaskin, J.F., Kazmer, D.J., 2009. Introgression between invasive saltcedars (*Tamarix chinensis* and *T. ramosissima*) in the USA. Biol. Inv. 11, 1121–1130.

Gelman, A., 2006. Prior distributions for variance parameters in hierarchical models (comment on article by Browne and Draper). Bayes. Anal. 1, 515–534.
Gelman, A., Rubin, D.B., 1992. Inference from iterative simulation using multiple sequences. Stat. Sci. 7, 457–472.
Grady, K.C., Ferrier, S.M., Kolb, T.E., Hart, S.C., Allan, G.J., Whitham, T.G., 2011. Genetic variation in productivity of foundation species at the edge of their distribution: implications for restoration and assisted migration. Glob. Change Biol. 17, 37243735.
Grady, K.C., Laughlin, D.C., Ferrier, S.M., Kolb, T.E., Hart, S.C., Allan, G.J., Whitham, T. G., 2013. Conservative leaf economic traits correlate with fast growth of genotypes of a foundation riparian species near the thermal maximum extent of its geographic range. Funct. Ecol. 27, 428–438.
Grady, K.C., Kolb, T.E., Ikeda, D.H., Whitham, T.G., 2015. A bridge too far: cold and pathogen constraints at assisted migration in riparian forests. Res Ecol 23, 811–820.
Granier, A., 1987. Evaluation of transpiration in a Douglas fir stand by means of sap flow measurements. Tree Physiol 3, 309–320.
Guo, J.S., Gear, L., Hultine, K.R., Koch, G.W., Ogle, K., 2020. Non-structural carbohydrate dynamics associated with antecedent stem water potential and air temperature in a dominant desert shrub. Plant Cell Environ. https://doi.org/10.1111/pce.13749.
Hartmann, H., Ziegler, W., Trumbore, S., 2013. Lethal drought leads to reduction in nonstructural carbohydrates in Norway spruce tree roots but not in the canopy. Funct. Ecol. 27, 413–427.
Hartmann, H., Trumbore, S., 2016. Understanding the roles of nonstructural carbohydrates in forest trees – from what we can measure to what we want to know. New Phytol 211, 386–403.
Horton, J.S., 1977. The development and perpetuation of the permanent tamarisk type in the phreatophyte zone of the Southwest. In: Symposium on the Importance, Preservation and Management of the Riparian Habitat, pp. 124–127.
Hultine, K.R., Koepke, D.F., Pockman, W.T., Fravolini, A., Sperry, J.S., Williams, D.G., 2006. Influence of soil texture on hydraulic properties and water relations of a dominant warm-desert phreatophyte. Tree Physiol 26, 313–323.
Hultine, K.R., Nagler, P.L., Morino, K., Bush, S.E., Burtch, K.G., Dennison, P.E., Glenn, E. P., Ehleringer, J.R., 2010. Sap-flux-scaled transpiration by tamarisk (*Tamarix* spp.) before, during and after episodic defoliation by the saltcedar leaf beetle (*Diorhabda carinulata*). Agric. For. Meteorol. 150, 1467–1475.
Hultine, K.R., Burtch, K.G., Ehleringer, J.R., 2013. Gender specific patterns of carbon uptake and water use in a dominant riparian tree species exposed to a warming climate. Global Change Biol 19, 3390–3405.
Hultine, K.R., Froend, R., Blasini, D., Bush, S.E., Karlinski, M., Koepke, D.F., 2020. Hydraulic traits that buffer deep-rooted plants from changes in hydrology and climate. Hydrol. Proc. 34, 209–222.
Ikeda, D.H., Max, T.L., Allan, G.J., Lau, M.K., Shuster, S.M., Witham, T.G., 2016. Genetically informed ecological niche models improve climate change predictions. Glob. Change Biol. 23, 164–176.
Kawecki, T.J., Ebert, D., 2004. Conceptual issues in local adaptation. Ecol. Lett. 7, 1225–1241.
Lee, S.R., Jo, Y.S., Park, C.H., Friedman, J.M., Olson, M.S., 2018. Population genomic analysis suggests strong influence of river network on spatial distribution of genetic variation in invasive saltcedar across the southwestern United States. Mol. Ecol. 27, 636–646.
Long, R., Bush, S.E., Grady, K.C., Smith, D., D'Antonio, C.M., Dudley, T.L., Fehlberg, S.D., Gaskin, J.F., Glenn, E.P., Hultine, K.R, 2017. Can local adaptation explain varying patterns of herbivory tolerance in a recently introduced tree / shrub in North America? Con. Physiol. https://doi.org/10.1093/conphys/cox016.
Monteith, J.L., Unsworth, M.H., 1990. Principles of Environmental Physics. Arnold, London.
Mote, P.W., Hamlet, A.F., Clark, M.P., Lattenmaier, D.P., 2005. Declining mountain snowpack in western North America. Bull. Am. Met. Soc. 86, 39–49.
Mote, P.W., Li, S., Lettenmaier, D.P., Xiao, M., Engel, R., 2018. Dramatic declines in snowpack in the western US. npj Clim. Atm. Sci. 1 (2) https://doi.org/10.1038/s41612-018-0012-1.
Oren, R., Sperry, J.S., Katul, G., Pataki, D.E., Ewers, B.E., Phillips, N., Schafer, K.V.R, 1999. Survey and synthesis of intra- and interspecific variation in stomatal sensitivity to vapour pressure deficit. Plant, Cell Environ 22, 1515–1526.
Parker, I.M., Rodriguez, J., Loik, M.E., 2003. An evolutionary approach to understanding the biology of invasions: local adaptation and general-purpose genotypes in the week *Verbascum Thapsus*. Con. Biol. 17, 59–72.
Plummer, M., 2003. JAGS: A program for analysis of Bayesian graphical models using Gibbs sampling. In: Proceedings of the 3rd international workshop on distributed statistical computing 2003 Mar 20, 124, pp. 1–10.
Plummer, M. 2019. RJAGS: Bayesian Graphical Models using MCMC. R package version 4-9. https://CRAN.R-project.org/package=rjags.
Plummer, M., Best, N., Cowles, K., Vines, K., 2006. CODA: convergence diagnosis and output analysis for MCMC. R News 6, 7–11.
Pockman, W.T., Sperry, J.S., 2000. Vulnerability to xylem cavitation and the distribution of Sonoran Desert vegetation. Am. J. Bot. 87, 1287–1299.
PRISM Climate Group (2015) Oregon State University. Available at: http://prism.oregonstate.edu/.
R Core Team, 2018. R: A language and environment for statistical computing. R Foundation for Statistical Computing, Vienna, Austria. URL. https://www.R-project.org/.
Seager, R., Ting, M, Held, I., Kushnir, Y., Lu, J., Vecchi, G., Huang, H.P., Harnik, N., Leetmaa, A., Lau, N.C., Li, C., Velez, J., Naik, N, 2007. Model projections of an imminent transition to a more arid climate in southwestern. North America. Science 316, 1181–1184.
Seager, R., Vecchi, G.A., 2010. Greenhouse warming and the 21st century hydroclimate of southwestern North America. Proc. Nat. Acad. Sci. 107, 21277–21282.
Sexton, J.P., McKay, J.K., Sala, A., 2002. Plasticity and genetic diversity may allow saltcedar to invade cold climates in North America. Ecol. Appl. 12, 1651–1660.
Sperry, J.S., Sullivan, J.E.M, 1992. Xylem embolism in response to freeze-thaw cycles and water stress in ring-porous, diffuse porous, and conifer species. Plant Physiol 100, 605–613.
Sperry, J.S., Adler, F.R., Campbell, G.S., Comstock, J.P., 1998. Limitation of plant water use by rhizosphere and xylem conductance: results from a model. Plant Cell Environ 21, 347–359.
Sperry, J.S., Hacke, U.G., 2002. Desert shrub water relations with respect to soil characteristics and plant functional type. Funct. Ecol. 16, 367–378.
Sperry, J.S., Hacke, U.G., Oren, R., Comstock, J.P., 2002. Water deficits and hydraulic limits to leaf water supply. Plant Cell Environ 25, 251–263.
Thompson, J.N., 1998. Rapid evolution as an ecological process. Trends Ecol. Evol. 13, 329–332.
Tixier, A., Gambetta, G.A., Godfrey, J., Orozco, J., Zwieniecki, M.J., 2019. Non-structural carbohydrates in dormant woody perennials; the tale of winter survival and spring arrival. Front. For. Glob. Change. https://doi.org/10.3389/ffgc.2019.00018.
Urban, J., Ingwers, M.W., McGuire, M.A., Teskey, R., 2017. Increase in leaf temperature opens stomata and decouples net photosynthesis from stomatal conductance in *Pinus taeda* and *Populus deltoids* x *nigra*. J. Exp. Bot. 68, 1757–1767.
Williams, W.I., Friedman, J.M., Gaskin, J.F., Norton, A.P., 2014. Hybridization of an invasive shrub affects tolerance and resistance to defoliation by a biological control agent. Evol. Appl. 7, 381–393.
Würth, M.K.R., Peláez-Riedl, S., Wright, S.J., Körner, C, 2005. Non-structural carbohydrate pools in a tropical forest. Oecologia 143, 11–24.